



## RESEARCH ARTICLES

### Clearance of $^{141}\text{Ce}$ -Labeled Microspheres from Blood and Distribution in Specific Organs following Intravenous and Intraarterial Administration in Beagle Dogs

MOTOKO KANKE\*, GUY H. SIMMONS, DANIEL L. WEISS†, BRACK A. BIVINS, and PATRICK P. DeLUCA\*

Received July 26, 1979, from the *College of Pharmacy, University of Kentucky, Lexington, KY 40506*. Accepted for publication March 3, 1980. \*Present address: *Kitasato University, Yokohama, Japan*. †National Research Council, National Academy of Sciences, Washington, DC 20418.

**Abstract** □ The clearance of  $^{141}\text{Ce}$ -labeled polystyrene divinylbenzene microspheres in the 3–12- $\mu\text{m}$  diameter size range following intravascular administration was found to be size dependent, with the larger spheres clearing the circulation most rapidly. With spheres of high specific activity, dynamic distribution in various organs was determined by continuous whole-body scanning for the 1st hr after administration and by static imaging at selected times thereafter up to 4 weeks. The 7- and 12- $\mu\text{m}$  spheres were filtered mechanically and retained for prolonged periods in the lungs, while the 3- and 5- $\mu\text{m}$  spheres localized and were retained in the liver and spleen. Localization of these smaller spheres appeared to be due to phagocytosis by cells of the reticuloendothelial system; with the 12- $\mu\text{m}$  spheres, there was no evidence of phagocytosis by the pulmonary macrophages of the reticuloendothelial system within 4 weeks postadministration. Intraarterially administered larger microspheres did not show any significantly different distribution patterns from those administered intravenously. Histological examination revealed occasional vascular engorgement about the site of multiple-sphere lodgment, but no destructive tissue phenomenon was apparent in relation to the lodgment of the microspheres.

**Keyphrases** □ Microspheres—cerium 141 labeled, clearance from blood and distribution in specific organs following intravenous and intraarterial administration, dogs □ Clearance— $^{141}\text{Ce}$ -labeled microspheres, clearance from blood following intravenous and intraarterial administration, dogs □ Distribution— $^{141}\text{Ce}$ -labeled microspheres, distribution in specific organs following intravenous and intraarterial administration, dogs

Particulate matter found in injectable fluids and drugs has been a cause of concern to both the pharmaceutical industry and the medical practitioner (1–9). Until recently, most research efforts were directed at the amounts, origins, and physical properties of the particulates in parenteral drugs (10–15). Removal of these contaminants with final filters significantly reduces the incidence of infusion phlebitis, a local inflammatory process associated with intravenous fluid administration (16–20). Although some reports suggested that foreign particulates in parenteral

fluids may be hazardous, relatively little is known about distribution, relocation, and tissue effects of particulates entering the vascular system.

The possible effects and fate of injected model particulate matter recently were evaluated methodically as a function of the size and number administered intravenously to beagle dogs (21, 22). Of the size ranges chosen for these studies (microspheres of 3, 8, 15, and 25  $\mu\text{m}$  in diameter), only the 3- $\mu\text{m}$  model particles appeared to clear the lung capillary bed after an initial retention period and eventually relocated in the liver and spleen where they remained indefinitely. Although the studies yielded useful information about the ultimate fate of the microspheres, no definitive information concerning the dynamics of this relocation was obtained.

Since the previous study showed that relocation was limited to the smaller spheres, the purpose of this investigation was to obtain a clearer understanding of the time dependency of the observed relocation of a narrower range of microspheres injected intravenously and intraarterially. Four microsphere sizes in the 3–12- $\mu\text{m}$  range were selected and were of higher specific activity than the ones used previously. Additionally, a more intensive histological examination was conducted on specific tissues at various intervals to assess the location of spheres, tissue loads, and possible tissue damage.

#### EXPERIMENTAL

**Microspheres**—Polystyrene divinylbenzene microspheres<sup>1</sup> labeled with cerium 141 were obtained as suspensions in normal saline. These

<sup>1</sup> Nuclear Products Division, 3M Co., St. Paul, Minn.

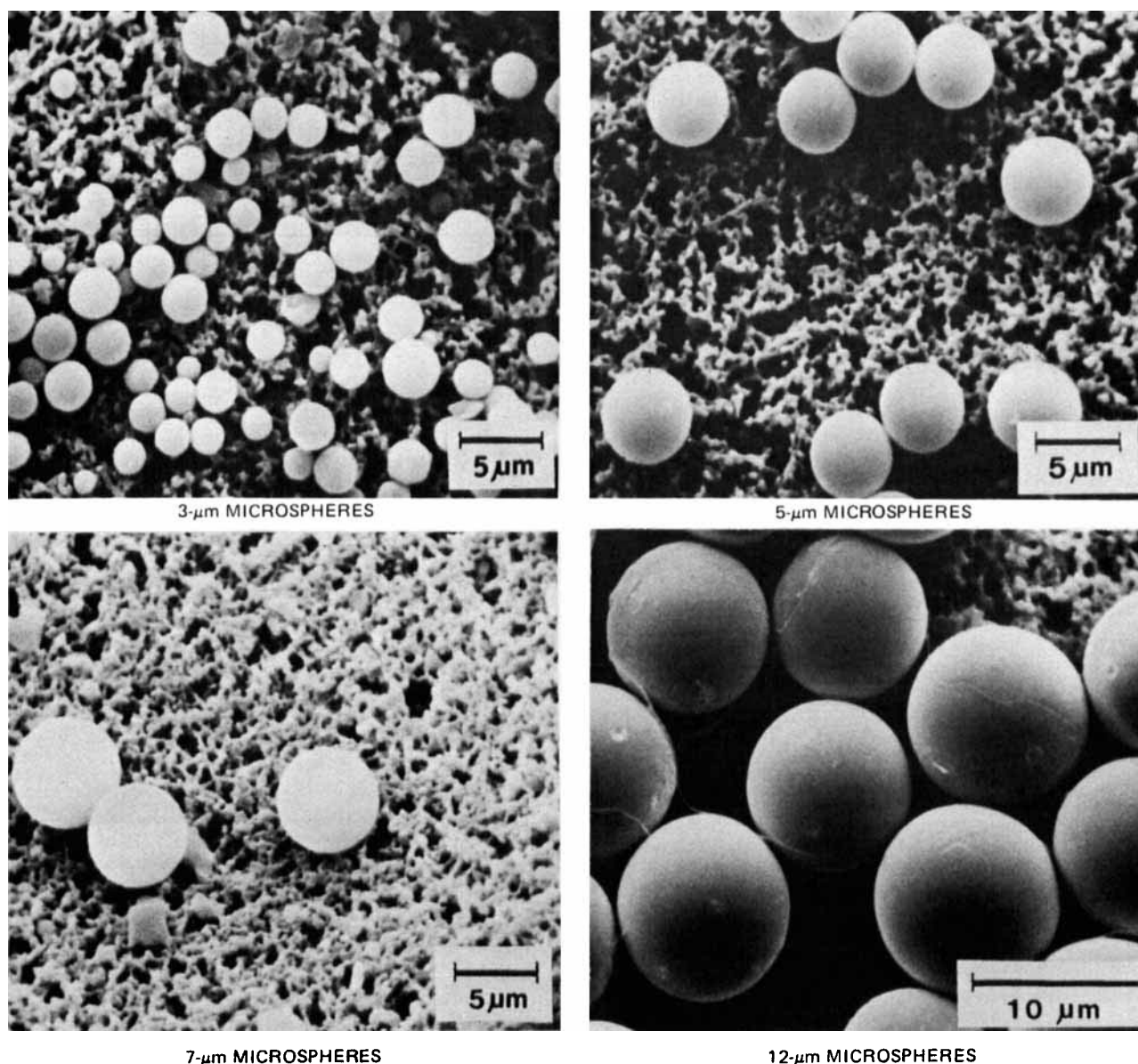


Figure 1—Scanning electron micrographs of polystyrene divinylbenzene microspheres labeled with cerium 141 at 20 kv (2400 $\times$  magnification).

microspheres are shown in the scanning electron microscope photomicrographs in Fig. 1. The specific activity was  $\sim 50$  mCi/g, five times higher than that used previously (21) to allow for more frequent scanning as well as blood level determinations using small blood samples. The size and number of spheres were controlled using an electronic particle counter<sup>2</sup> and microscopic<sup>3</sup> monitoring.

The permanency of the radioactive tag was checked by filtration of a sample using a  $0.45\text{-}\mu\text{m}$  filter and monitoring of the filtrate for activity. Additionally, urine and feces excreted from the first dog of each sphere-size group were collected during the 1st day and analyzed for radioactivity. Analysis of the filtrate and excreta confirmed the permanency of the radioactive tag.

**Dose Preparation**—Following ultrasonic treatment of the spheres for at least 5 min as well as occasional agitation by hand, doses were drawn into a syringe; the radioactivity was checked with a radioisotope calibrator<sup>4</sup> prior to administration.

**Preparation of Experimental Animals**—The beagle dogs were 2–3-year-old purebred females weighing 8.1–12.5 kg. The dogs were anesthetized with pentobarbital sodium at a dose of 30 mg/kg iv, and a 20-gauge needle equipped with a three-way stopcock was inserted into the radial veins of the left and right forelegs for intravenous dosing and

blood sampling, respectively. For intraarterial administration, a cannula was threaded from the common carotid artery into the left ventricle. The placement of the cannula was verified by demonstration of a left ventricular pressure curve *via* a transducer-recorder hookup.

Each dog was restrained in a supine position on a hard board, placed under a scintillation camera<sup>5</sup>, and positioned to align the chest and abdomen for imaging. After completion of imaging, the dogs that had a cannula inserted were given antibiotic prophylaxis with penicillin G procaine at 400,000–1,000,000 units/day im for 1–3 days.

**Dose Administration**—The size and number of microspheres administered to the beagle dogs are listed in Table I. The prepared dose of microspheres was administered directly from the syringe through the stopcock over 2 min. The syringe and cannula were flushed with 20 ml of sterile water for injection through the stopcock, completing the injection.

Animals were sacrificed at 20 min, 1 hr, 24 hr, or 4 weeks after administration.

**Mode of Imaging**—For whole-body scanning, the scintillation camera was interfaced to a digital computer<sup>6</sup>. Immediately following dosing, serial images of the chest and abdomen were recorded at the rate of 12 frames/min for the first 2 min followed by 2 frames/min for the next 58 min. Delayed static images were recorded at 2 and 24 hr and 1, 2, and 4

<sup>2</sup> Coulter counter model TALL, Coulter Electronics, Hialeah, Fla.

<sup>3</sup> Zetopan Universal Research Microscope, Riechert, Austria.

<sup>4</sup> Model CRC-6A, E. R. Squibb & Sons, East Brunswick, N.J.

<sup>5</sup> Pho/Gamma LFOV, Searle Radiographics, Des Plaines, Ill.

<sup>6</sup> PDP-1140, Digital Equipment Corp., Maynard, Mass.

**Table I—Size of Microspheres Administered and Dosage Range**

Number of Dogs	Sphere Size, $\mu\text{m}$	Dosage Range	
		Radioactivity, $\mu\text{Ci}$	Number of Spheres <sup>a</sup> , $\times 10^6$
9	$3.4 \pm 0.7$	244–838	253–890
8	$5.4 \pm 0.5$	505–806	73–101
5	$7.4 \pm 0.5$	571–1192	46–93
5	$11.6 \pm 0.5$	409–538	8.6–10

<sup>a</sup> Number of spheres per milligram =  $(1.55 \times 10^9)/D^3$ , where  $D$  is the mean sphere diameter in microns.

weeks following microsphere administration. All data were stored on magnetic tapes for review and analysis.

**Determination of Distribution**—Microsphere distributions were determined externally by flagging individual organs using computer-generated images and integrating the counts within each flagged area.

Specific intact organs, including the lungs, liver, spleen, heart, kidneys, brain, and tongue, were removed following sacrifice and scanned individually with the scintillation camera to quantitate the distribution at specific times. Efficiency values with units of counts per minute per mi-

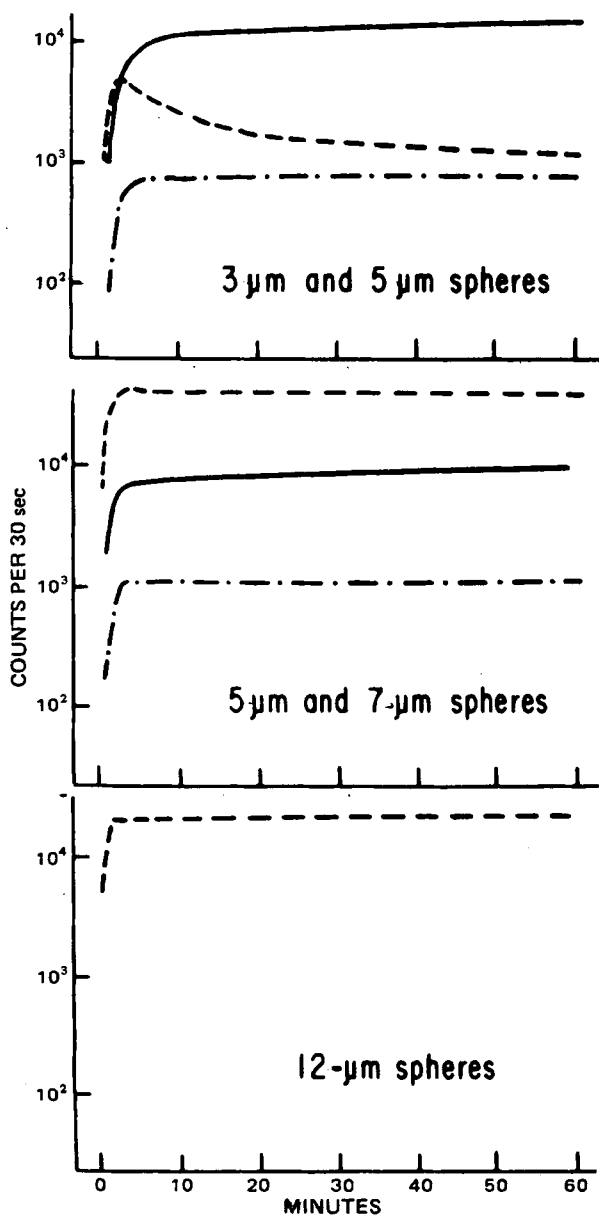


**Figure 2**—Distribution patterns of microspheres obtained by rapid frame sequential scanning during the first 60 min following administration. Count rates were corrected for differences in administered activity. Key: —, liver; --, lung; and - · -, spleen.

**Table II—Tissues for Histological Study**

Organ	Specific Tissue
Heart	Right ventricle, left ventricle
Lungs	Right middle lobe, right lower lobe, left lower lobe, left upper lobe
Liver	Right lobe, left lobe
Spleen	Including capsule
Kidneys	Right including capsule and pelvis, left including capsule and pelvis
Bone marrow	Squeezing of one rib for marrow sample
Brain	Left cortex
Peripheral blood	Direct blood smear immediately after injection, direct blood smear immediately before sacrifice, buffy coat immediately after injection, buffy coat immediately before sacrifice
Tongue	

crocurie were determined for each organ by adding a known amount of radioactivity to a plastic bag filled with an amount of water equivalent to the mass of the organ. The bag was shaped to simulate the shape of the organ and scanned in the same geometry as the excised organ.

Following the intact organ scanning, small specimens were removed from each organ for histological examination, and the remainder of the organ then was homogenized with a known amount of distilled water in a blender<sup>7</sup>. A 5-ml rubber-top container<sup>8</sup> was 70% filled with an aliquot of the homogenized sample and weighed. One to five samples were prepared for each organ and analyzed using a well-type  $\gamma$ -counter<sup>9</sup>. The counter efficiency was determined beforehand utilizing a known amount of radioactivity.

**Blood Level Determination**—Approximately 1–2 ml of venous blood was removed immediately after dose administration and at frequent intervals during the initial stage of each run. Total emissions of a weighed

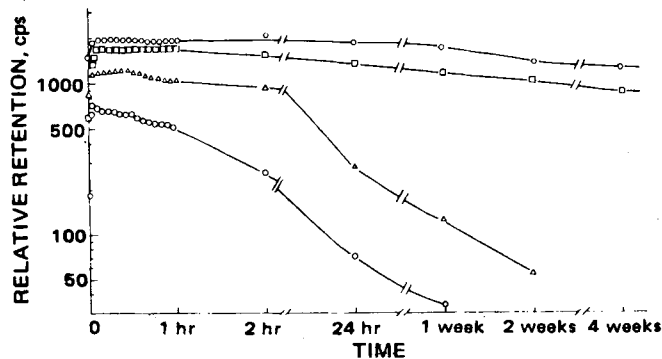


**Figure 3**—Relative retention and average time dependence of microspheres in beagle dog lungs obtained by external scanning following intravenous administration based on a 500- $\mu\text{Ci}$  dose. Key:  $\circ$ , 3- $\mu\text{m}$  spheres;  $\Delta$ , 5- $\mu\text{m}$  spheres;  $\square$ , 7- $\mu\text{m}$  spheres; and  $\diamond$ , 12- $\mu\text{m}$  spheres.

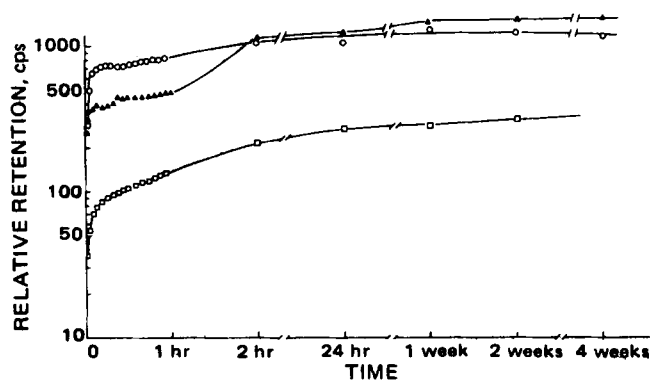


**Figure 4**—Relative retention and average time dependence of microspheres in beagle dog liver obtained by external imaging following intravenous administration based on a 500- $\mu\text{Ci}$  dose. Key:  $\circ$ , 3- $\mu\text{m}$  spheres;  $\Delta$ , 5- $\mu\text{m}$  spheres; and  $\square$ , 7- $\mu\text{m}$  spheres.

<sup>7</sup> Waring model 5011.

<sup>8</sup> Vacutainer.

<sup>9</sup> Model 4 spectroscaler, Picker Nuclear Corp., Northford, Conn.

**Table III—Quantitative Recovery of Radioactivity (Percent) in Individually Scanned Intact Organs following Intravenous (IV) and Intraarterial (IA) Administration**

Organ	3- $\mu$ m Spheres		5- $\mu$ m Spheres		7- $\mu$ m Spheres		12- $\mu$ m Spheres	
	IV	IA	IV	IA	IV	IA	IV	IA
<b>Sacrificed 20 min after Administration</b>								
Heart	0	0.1						
Lungs	23.7	22.7						
Liver	54.6	49.2						
Spleen	14.3	9.3						
Kidneys	0	1.9						
Brain	0	0.1						
Total recovery	92.6	83.3						
<b>Sacrificed 1 hr after Administration</b>								
Heart	0.3	0.3						
Lungs	21.1	9.4						
Liver	60.1	69.7						
Spleen	8.2	7.0						
Kidneys	0.2	1.7						
Brain	0.1	0.1						
Total recovery	90.0	88.2						
<b>Sacrificed 24 hr after Administration</b>								
Heart	0	2.6 <sup>a</sup>						
Lungs	1.4	4.2						
Liver	70.5	72.7						
Spleen	7.4	8.3						
Kidneys	0	0.3						
Brain	0	0.4						
Tongue								
Total recovery	79.3	88.5						
<b>Sacrificed 4 Weeks after Administration</b>								
Heart	0	0.1						
Lungs	5.0	1.1						
Liver	69.2	74.8						
Spleen	13.6	8.4						
Kidneys	0	0						
Brain	0	0						
Tongue								
Total recovery	87.8	84.4						

<sup>a</sup> Obtained at 14 hr.

blood sample were counted by a well-type  $\gamma$ -counter for 10 min.

**Histological Evaluation**—Specific tissue specimens,  $\sim 10 \times 20 \times 3$  mm, were cut from the organs listed in Table II. The tissues were processed through formaldehyde fixation, paraffin embedding, and staining

with hematoxylin and eosin. Slide preparations 5–14  $\mu$ m thick were prepared, depending on the size of the microspheres. Direct blood smears and buffy coat smears were prepared with blood samples obtained immediately after dose administration and immediately before sacrifice.

**Table IV—Quantitative Recovery of Radioactivity (Percent) in Homogenized Organs following Intravenous (IV) and Intraarterial (IA) Administration**

Organ	3- $\mu$ m Spheres		5- $\mu$ m Spheres		7- $\mu$ m Spheres		12- $\mu$ m Spheres	
	IV	IA	IV	IA	IV	IA	IV	IA
<b>Sacrificed 20 min after Administration</b>								
Heart	0.3	0.1						
Lungs	15.9	19.3						
Liver	41.6	38.0						
Spleen	10.8	6.6						
Kidneys	0.1	1.5						
Total recovery	68.7	65.5						
<b>Sacrificed 1 hr after Administration</b>								
Heart	0.2	0.2						
Lungs	15.5	9.5						
Liver	49.0	61.6						
Spleen	7.3	7.1						
Kidneys	0.1	0.6						
Total recovery	72.1	79.0						
<b>Sacrificed 24 hr after Administration</b>								
Heart	0.1	1.8 <sup>a</sup>						
Lungs	1.2	3.5						
Liver	62.5	52.9						
Spleen	6.0	5.4						
Kidneys	0	0.2						
Total recovery	69.8	63.8						
<b>Sacrificed 4 Weeks after Administration</b>								
Heart	0	0.1						
Lungs	4.4	0.9						
Liver	52.1	68.0						
Spleen	10.5	7.4						
Kidneys	0	0.6						
Total recovery	67.0	77.0						

<sup>a</sup> Obtained at 14 hr.

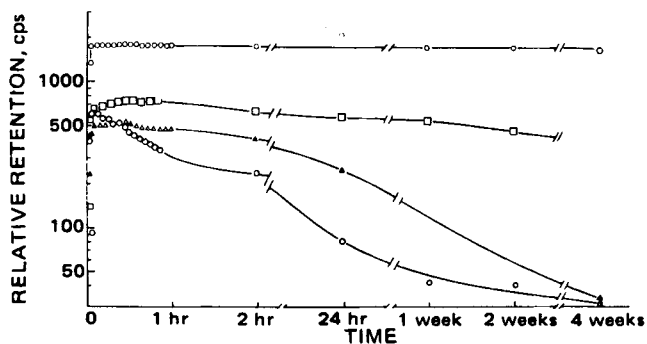


**Figure 5**—Relative retention and average time dependence of microspheres in beagle dog lungs obtained by external scanning following intraarterial administration based on a 500- $\mu$ Ci dose. Key:  $\circ$ , 3- $\mu$ m spheres;  $\Delta$ , 5- $\mu$ m spheres;  $\square$ , 7- $\mu$ m spheres; and  $\circ$ , 12- $\mu$ m spheres.

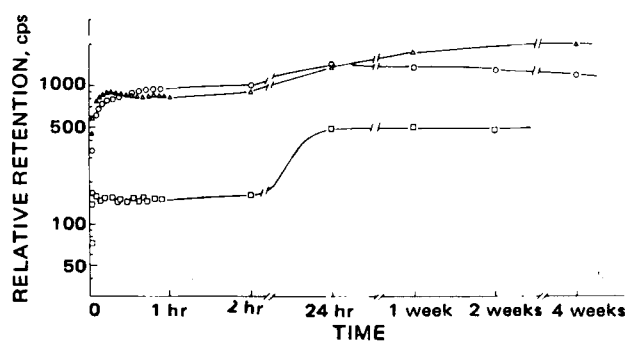


**Figure 6**—Relative retention and average time dependence of microspheres in beagle dog liver obtained by external scanning following intraarterial administration based on a 500- $\mu$ Ci dose. Key:  $\circ$ , 3- $\mu$ m spheres;  $\Delta$ , 5- $\mu$ m spheres; and  $\square$ , 7- $\mu$ m spheres.

## RESULTS

**Distribution Patterns**—Whole-body scanning showed that almost all of the radioactivity was localized in the central region, with especially

high concentrations in the lungs, liver, and spleen. A set of typical temporal distribution curves for these three organs obtained from rapid frame sequential scanning for the first 60 min is shown in Fig. 2. Although the curves were corrected for differences in administered activity, due to the

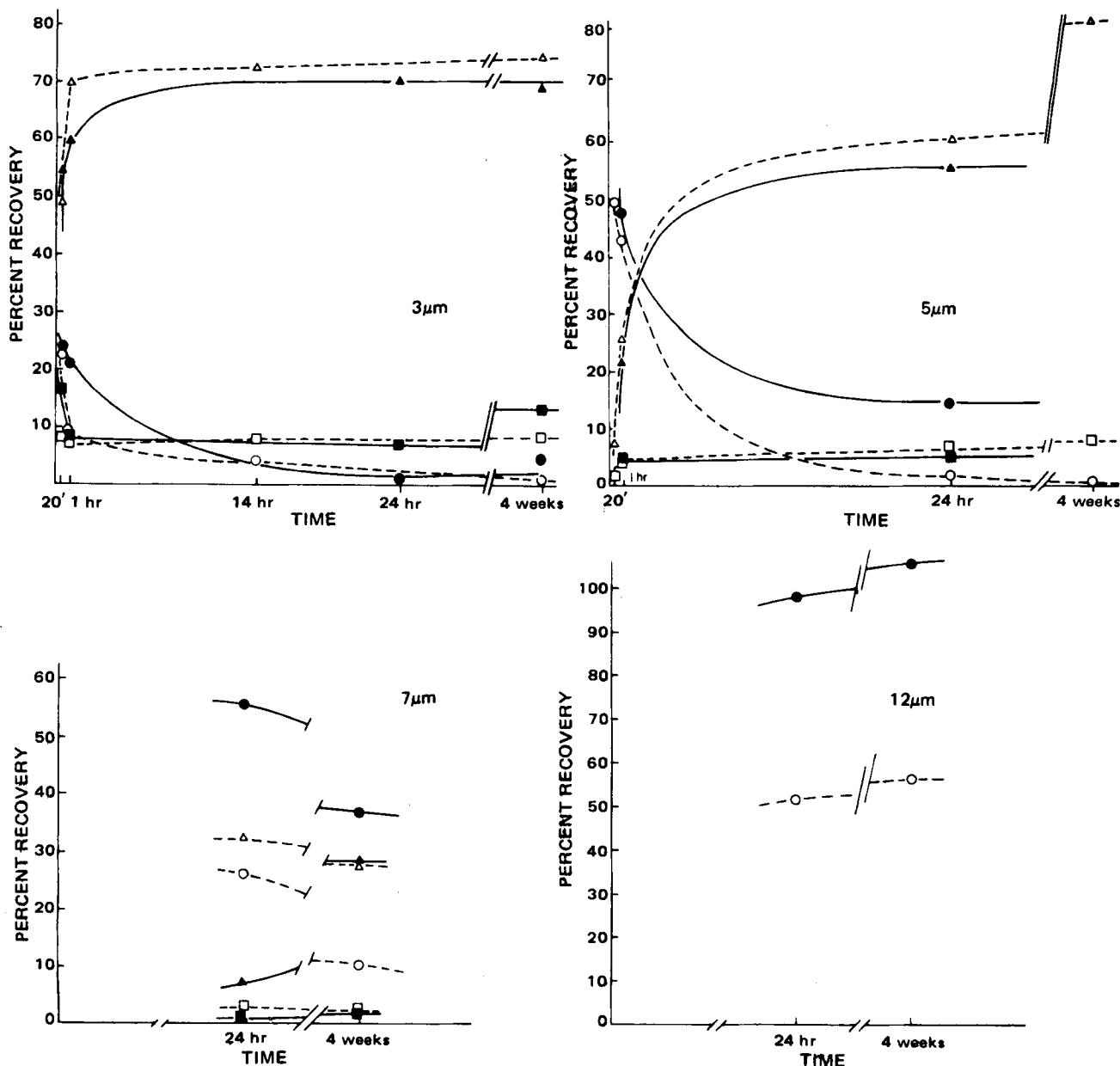


**Figure 7**—Quantitative recovery of microspheres in individually scanned intact organs. Key:  $\Delta$ ,  $\Delta$ , liver;  $\bullet$ ,  $\circ$ , lungs; and  $\blacksquare$ ,  $\square$ , spleen; closed symbols represent intravenous administration, and open symbols represent intraarterial administration.

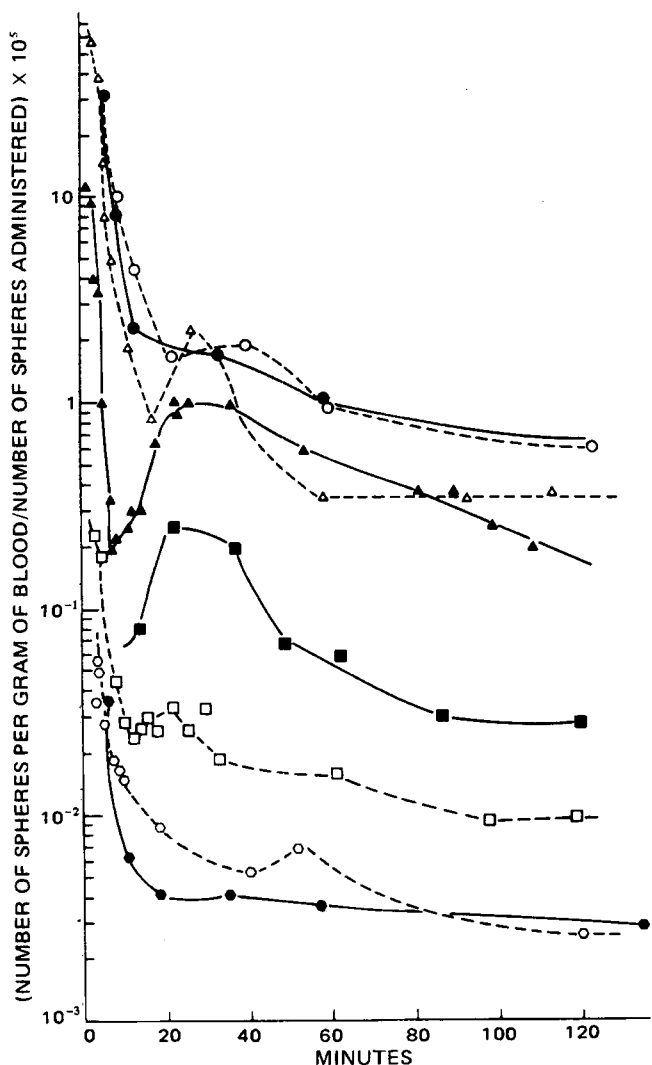


**Figure 8**—Ratio of the number of spheres per gram of blood to that administered as a function of time. Key: ●, ○, 3- $\mu$ m spheres; ▲, △, 5- $\mu$ m spheres; ■, □, 7- $\mu$ m spheres; and ●, ○, 12- $\mu$ m spheres; closed figures and solid lines represent intravenous administration, and open figures and broken lines represent intraarterial administration.

difficulty in isolating entire organ profiles resulting from organ overlap, only relative counts and not absolute uptake values are shown. However, the curves demonstrate the general distribution over the first 60 min.

No clearcut difference in distribution patterns was observed between intravenous and intraarterial administration of microspheres. With the 3- $\mu$ m microspheres injected in nine dogs, there was an initial distribution to the lungs followed by rapid clearance from the lungs and localization in the liver and spleen. Six of eight dogs injected with 5- $\mu$ m spheres exhibited similar lung patterns. With the 7- $\mu$ m microspheres, retention in the lungs was greater and clearance was more gradual in all five dogs injected. On the other hand, all of the 12- $\mu$ m microspheres were retained in the lungs.

Following the dynamic imaging for the initial 60 min, static images were recorded from the live animal at 2 and 24 hr and 1, 2, and 4 weeks after dose administration. The relative retention curves for the lungs and liver following either intravenous or intraarterial administration obtained by such external imaging are shown in Figs. 3–6. The 12- $\mu$ m microspheres distributed only to the lungs regardless of the administration route and were retained in the lung area even at 4 weeks after administration.

**Quantitative Determination of Distribution**—Following sacrifice, specific organs including the lungs, liver, spleen, heart, kidneys, brain, and tongue were removed and scanned by the scintillation camera. The results are listed in Table III and plotted in Fig. 7. The analyzed data of uniformly homogenized organs are listed in Table IV.

The 3- $\mu$ m spheres were cleared from the lungs and localized in the liver much more readily than the 5- $\mu$ m spheres. Within 24 hr, >95% of the 3- and 5- $\mu$ m spheres appeared to have passed from the lungs of all dogs

except one of the 5- $\mu$ m group, where 12–14% of the microsphere dose was retained in the lungs. Clearance of the 7- $\mu$ m spheres from the lungs following intravenous administration was much slower than that with the smaller sizes. After 24 hr, over 43% of the dose was still in the lungs and only 7% had localized in the liver. However, after 4 weeks, only 26–37% of the microspheres administered intravenously remained in the lungs, and the level in the liver increased to 20–28%. The 12- $\mu$ m spheres were not detected outside of the lungs after 24 hr following intravenous administration in dogs that were followed for up to 4 weeks.

There were no significant differences in distribution of the 3- and 5- $\mu$ m spheres between intravenous and intraarterial administration, but some differences were observed with larger spheres. The 12- $\mu$ m spheres administered intraarterially were retained in the lungs for at least 4 weeks. A major difference between the intravenous and intraarterial administration with the 12- $\mu$ m size was that some spheres were detected in the brain and tongue after intraarterial administration.

The results obtained from the two quantitative recovery methods were reasonably close to each other. Therefore, the quantitative determination by imaging the intact organs was chosen as being easier and quicker than the homogenized method.

**Blood Levels**—Figure 8 shows the typical blood levels of the microspheres over a 2-hr period following intravenous or intraarterial administration. Elimination of spheres from the circulating blood pool appeared to be size dependent and more rapid with larger sizes. The blood levels of 12- $\mu$ m spheres were essentially the same as background levels within 2 hr after administration, while the 3- $\mu$ m spheres recirculated longer and maintained higher blood levels than did the larger sizes. The number of spheres administered within the size and volume ranges tested appeared to have no effect on the elimination rate from the blood.

Most curves in Fig. 8 show an increase in blood activity between 10 and 30 min after administration. This phenomenon is not explained easily, and more frequent blood sampling is required to define this portion of the curves.

**Histology Data**—A histological study of representative tissue samples from multiple organs was undertaken (Table II). Identification of microspheres was facilitated by examination under green and red filtered light. Under these conditions (Fig. 9), the microspheres appear as dense black spheres of smooth regular outline. Therefore, the spheres may be distinguished from cell nuclei, even when samples containing smaller spheres of approximately the same diameter as cell nuclei are evaluated.

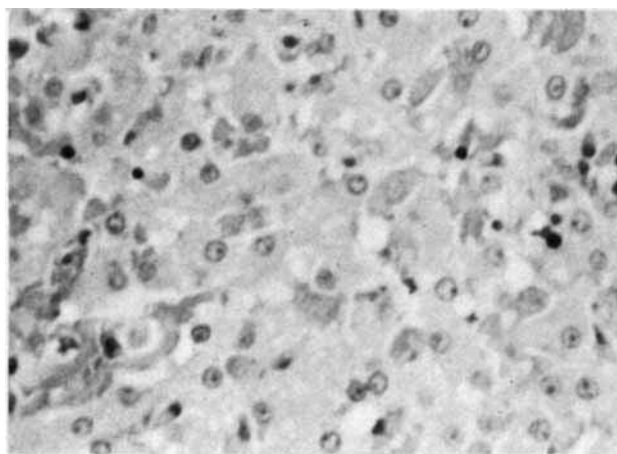
Individual 3- and 5- $\mu$ m microspheres were found consistently in vascular channels, Kupffer cells, and the sinusoids of the liver, spleen, and bone marrow within phagocytizing cells. The cells were vascular endothelium, monocytoic phagocytes, or cells of the reticuloendothelial system. There was moderate engorgement of the sinusoids, which were slightly distended and congested. No multinucleated giant cells appeared to participate in the phagocytic activity.

Larger microspheres and clusters of smaller spheres generally lay free in vascular and sinusoidal channels. A few 7- $\mu$ m microspheres were phagocytized, but these microspheres represented <10% of the total tissue loads. Figure 9c shows three single spheres within slightly distended Kupffer cells. The histology of the liver is inconspicuous except for mild congestion. Figure 9d shows a single 12- $\mu$ m sphere lodged in the pulmonary capillary, and slight engorgement of pulmonary vasculature is evident. The buffy coat smears were all negative, with two exceptions: one dog administered 3- $\mu$ m spheres and one administered 5- $\mu$ m spheres showed one and two spheres, respectively, in their buffy coats obtained immediately after injection. While this finding attests to the validity of the procedure, it does not provide information on the subsequent distribution characteristics.

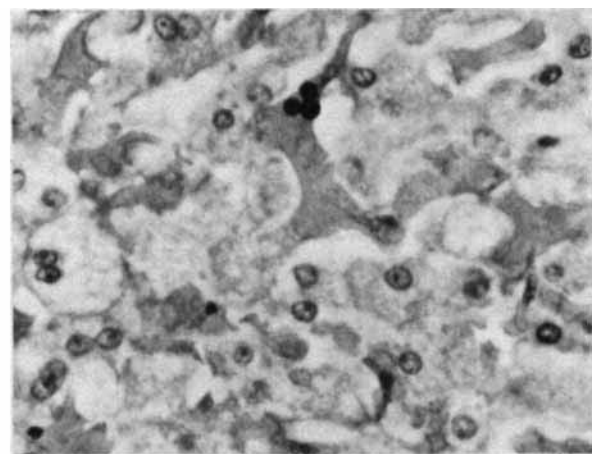
Although occasional vascular engorgement was present around the site of multiple-sphere lodgment and may represent a local hemodynamic response to partial blockage of the vascular channels, destructive tissue phenomena were not seen in relation to the lodgment of the microspheres.

## DISCUSSION

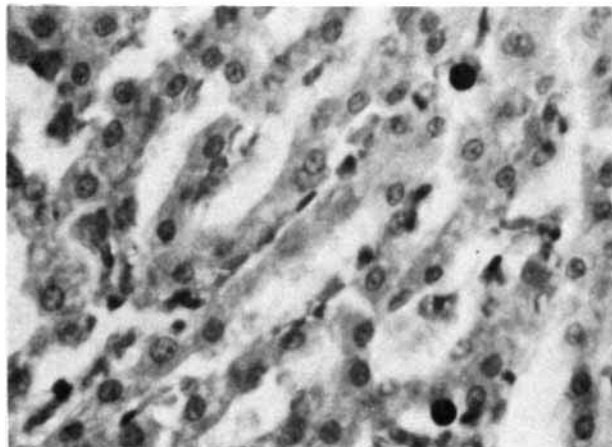
These studies confirm that clearance of microspheres from the blood following intravascular injection is size dependent, with the larger diameter spheres clearing most rapidly (Fig. 8). The initial clearance appears to be due to a simple filter effect of the pulmonary capillary beds, although vascular constriction and venous sphincters may play some role in the trapping process. Spheres of 7- $\mu$ m diameter and larger initially were retained in the lungs, while large numbers of the 3- and 5- $\mu$ m spheres



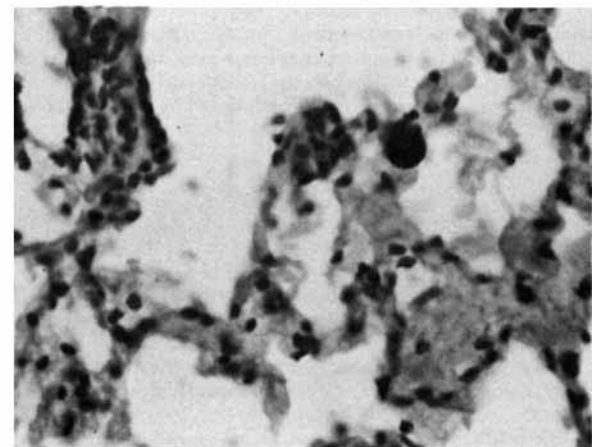
a, DOG 3, LIVER, 3.4  $\mu\text{m}$



b, DOG 15, LIVER, 5.4  $\mu\text{m}$



c, DOG 11, LIVER, 7.4  $\mu\text{m}$



d, DOG 23, LUNG, 11.6  $\mu\text{m}$

**Figure 9**—Photomicrographs of tissue samples. Key: a, 3- $\mu\text{m}$  spheres in liver; b, 5- $\mu\text{m}$  spheres in liver; c, 7- $\mu\text{m}$  spheres in liver; and d, 12- $\mu\text{m}$  spheres in lungs. Obtained with hematoxylin and eosin stain (160 $\times$ ).

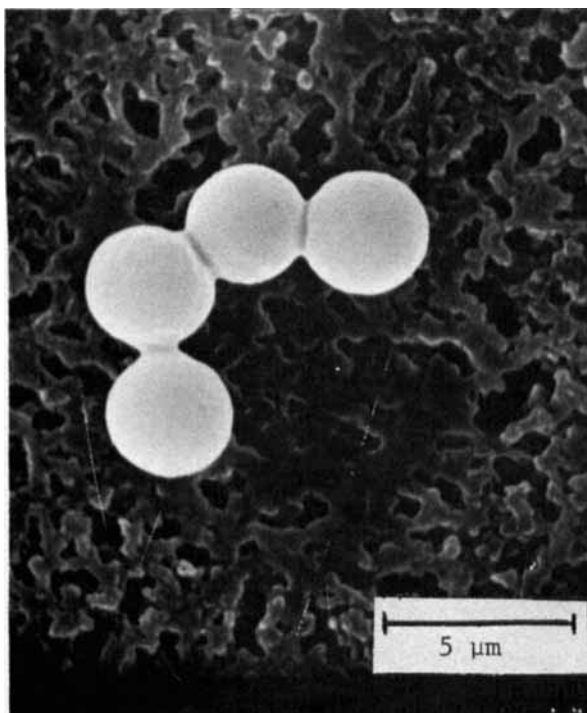


**Figure 10**—Scanning electron photomicrograph of 3- $\mu\text{m}$  microspheres from a venous blood sample 1 hr following administration at 20 kv (5000 $\times$  magnification).

passed through, implying a critical circulation diameter for nondeformable particles reaching the pulmonary vascular bed.

The increase in blood activity seen between 10 and 30 min following administration of the spheres may be due to washout within the lungs so that spheres initially trapped are washed through opening arteriovenous shunts to recirculate in the bloodstream (Fig. 8). Although 98–99% of the spheres were cleared from the circulation in 10–30 min, blood sampling over the first 2 hr following administration revealed concentrations of  $10^4$  3- $\mu\text{m}$  spheres, 100–1000 5- $\mu\text{m}$  spheres, 10–100 7- $\mu\text{m}$  spheres, and less than one 12- $\mu\text{m}$  sphere/g of blood. The possible association of the spheres with circulating blood cells warrants further attention and will be undertaken with more sophisticated scanning electron microscopic procedures.

Distribution patterns varied with the sphere size studied and became complex over time. With the 3- $\mu\text{m}$  spheres and in six of eight dogs with the 5- $\mu\text{m}$  spheres, there was initial distribution to the lungs followed by rapid clearance, with localization and retention in the liver and spleen peaking within 20 min of administration for the 3- $\mu\text{m}$  spheres and within 24 hr for the 5- $\mu\text{m}$  spheres (Tables III and IV). This retention is explained by the histological observation of phagocytosis of the 3- and 5- $\mu\text{m}$  spheres by the Kupffer cells of the liver and the sinusoidal lining of the spleen (23, 24).

Clearance of the 7- $\mu\text{m}$  spheres from the lungs to the liver and spleen occurred much more slowly, with 26–37% remaining in the lungs at 4 weeks. This slow migration may be due to retention in the lungs with phagocytosis by pulmonary macrophages and subsequent migration to the reticuloendothelial system. The 12- $\mu\text{m}$  spheres were retained in the lungs from the initial injection throughout the study. Failure of the 12- $\mu\text{m}$  spheres to undergo phagocytosis and relocation may indicate a size limit for phagocytosis of inert particles (25).

No clearcut differences in the clearance or distribution of the 3- and 5- $\mu\text{m}$  spheres were observed between intraarterial and intravenous administration (Fig. 8 and Tables III and IV). For reasons that are not clear, these spheres either passed through or did not enter muscular or visceral

beds following intraarterial administration and recirculated as if they had been injected into the venous system. Minimal differences were seen between intravenous and intraarterial administration of the larger spheres, but 12- $\mu\text{m}$  spheres were detected in the brain and tongue following intraarterial administration. These observations were contrary to expectations and suggest that the flow characteristics of the spheres are such that distribution to peripheral and visceral capillary beds is limited.

In many cases, the 3- $\mu\text{m}$  spheres were seen microscopically to lodge in the studied tissues as agglomerated masses of three to 10 spheres. This property was observed less frequently with the 5- $\mu\text{m}$  spheres and not at all with the 7- and 12- $\mu\text{m}$  spheres. The light microscopy observations did not indicate any significant damage of cells containing the spheres at the substructural or functional levels. Progress in answering these questions will depend on enzyme biochemistry and electron microscopy studies.

Figure 10 shows a cluster of 3- $\mu\text{m}$  microspheres from a venous blood sample obtained 1 hr after administration. Although further investigation is required to clarify this clustering phenomenon, the microspheres may become coated with blood proteins with sticky characteristics and may adsorb platelets on their surface (26-28)<sup>10</sup>. Clustering by surface to surface protein adhesion would be facilitated by slow flow through the capillary and sinusoidal beds and by the high surface to mass ratio of the smaller spheres. Contact among larger spheres may be limited by the diameter of the vascular channels, while the smaller surface to mass ratio may limit the mutual adherence potential exhibited by the 3- and 5- $\mu\text{m}$  spheres.

### CONCLUSIONS

1. Elimination of microspheres from the circulation following intravascular administration is size dependent, with the larger diameter spheres clearing most rapidly.
2. Mechanical filtration and prolonged retention of 7- $\mu\text{m}$  and larger spheres in the lungs imply a critical size for passage through the pulmonary vascular bed.
3. Retention of small microspheres (3 and 5  $\mu\text{m}$ ) in the liver and spleen for prolonged periods appears to be due to phagocytosis of the spheres by cells of the reticuloendothelial system.
4. Small microspheres (3  $\mu\text{m}$ ) tend to agglomerate when administered intravascularly, presumably due to protein adherence and a large surface to mass ratio.
5. Intraarterially administered larger microspheres do not distribute to peripheral and visceral beds differently from the intravenous administration, presumably because of flow characteristics inhibiting peripheral distribution.
6. Large microspheres (12  $\mu\text{m}$ ) are not phagocytized by pulmonary macrophages or the reticuloendothelial system within 4 weeks of intravascular administration as are smaller sphere sizes, implying a size limit for phagocytosis of inert particles.

### REFERENCES

- (1) B. E. Konwaler, *Am. J. Clin. Pathol.*, **20**, 385 (1950).

- (2) E. J. Bruning, *Virchows Arch.*, **327**, 460 (1955).
- (3) S. Sarrut and C. Nezelof, *Presse Med.*, **68**, 375 (1960).
- (4) J. M. Garvan and B. W. Gunner, *Med. J. Aust.*, **2**, 140 (July 22, 1963).
- (5) *Ibid.*, **2**, 1 (July 4, 1964).
- (6) W. C. Walter, presented at the Food and Drug Administration Symposium on Safety of Large Volume Parenteral Solutions, Washington, D.C., July 1966.
- (7) M. J. Groves, *J. Hosp. Pharm.*, **25**, 17 (1968).
- (8) N. M. Davis, S. Turco, and E. Sively, *Am. J. Hosp. Pharm.*, **27**, 822 (1970).
- (9) S. Turco and N. M. Davis, *Hosp. Pharm.*, **8**, 137 (1973).
- (10) M. Sokol and J. Boyd, *Bull. Parenter. Drug Assoc.*, **22**, 9 (1968).
- (11) B. Trasen, *ibid.*, **22**, 1 (1968).
- (12) M. J. Groves and J. F. Major, *Pharm. J.*, **193**, 227 (1964).
- (13) Y. S. Lim, S. Turco, and N. M. Davis, *Am. J. Hosp. Pharm.*, **30**, 518 (1973).
- (14) J. Y. Masuda and J. H. Beckerman, *ibid.*, **30**, 72 (1973).
- (15) P. P. DeLuca, R. P. Rapp, B. A. Bivins, and T. Rebagay, *ibid.*, **33**, 433 (1976).
- (16) D. W. Wilmore and S. J. Dudrick, *Arch. Surg.*, **99**, 462 (1969).
- (17) P. B. Ryan, R. P. Rapp, P. P. DeLuca, W. O. Griffen, J. D. Clark, and D. Cloys, *Bull. Parenter. Drug Assoc.*, **27**, 1 (1973).
- (18) P. P. DeLuca, R. P. Rapp, B. A. Bivins, H. E. McKean, and W. O. Griffen, *Am. J. Hosp. Pharm.*, **32**, 1001 (1975).
- (19) H. G. Schroeder and P. P. DeLuca, *ibid.*, **33**, 543 (1976).
- (20) B. A. Bivins, R. P. Rapp, P. P. DeLuca, H. McKean, and W. O. Griffen, *Surgery*, **85**, 388 (1979).
- (21) H. G. Schroeder, G. H. Simmons, and P. P. DeLuca, *J. Pharm. Sci.*, **67**, 504 (1978).
- (22) H. G. Schroeder, B. A. Bivins, G. P. Sherman, and P. P. DeLuca, *ibid.*, **67**, 508 (1978).
- (23) M. D. Schoenberg, P. A. Gilman, V. R. Mumaw, and R. D. Moore, *Br. J. Exp. Pathol.*, **42**, 486 (1961).
- (24) J. M. Singer, L. Adlersberg, E. M. Hoenig, E. Ende, and Y. Tchorsch, *J. Reticuloendothel. Soc.*, **6**, 561 (1969).
- (25) B. Holma, *Acta Med. Scand.*, **473**, 1 (1967).
- (26) R. E. Baier and R. C. Dutton, *J. Biomed. Mater. Res.*, **3**, 43 (1969).
- (27) D. E. Scarborough, R. G. Mason, T. G. Galldox, and K. M. Brinkhaus, *Lab. Invest.*, **20**, 164 (1969).
- (28) M. A. Packhan, G. Evans, M. F. Glynn, and J. F. Mustard, *J. Lab. Clin. Med.*, **73**, 686 (1969).

### ACKNOWLEDGMENTS

Presented at the Basic Pharmaceutics Section, APhA Academy of Pharmaceutical Sciences, Hollywood, Fla. meeting, November 1978.

Supported by Contract 223-77-3018 from the Public Health Service, Food and Drug Administration, Department of Health, Education, and Welfare.

The authors thank Dr. Irena Sniecinski for assistance and consultation with the histological evaluation and Mr. C. Cheng for assistance with the animal studies.

<sup>10</sup> Confirmed by S. W. Kim, College of Pharmacy, University of Utah, personal communication.